Scientific Contributions Oil & Gas, Vol. 49. No. 2, June: 593 - 608

SCIENTIFIC CONTRIBUTIONS OIL AND GAS

Testing Center for Oil and Gas
LEMIGAS

Journal Homepage:http://journal.lemigas.esdm.go.id
ISSN: 2089-3361, e-ISSN: 2541-0520

Pseudo-3D Depth Reconstruction from Multi-Vintage 2D and 3D Seismic Data in The Offshore Southeast Sumatra

Dadang Ramdan[1], Abdul Haris[1], Dewi Manik Darmayanti[2], Permana Citra Adi[2], Iwan Rudiyanto[2], and Muhamad Yanuar Mahardi[2]

[1]Universitas Indonesia,
Master of Physics Program, Pondok Cina, Beji, Depok, Indonesia.

[2]Pertamina EP
RDTX Square, Semanggi, Setiabudi, Jakarta, Indonesia.

Corresponding author: Dadang Ramdan (da.ramdan@gmail.com)

Manuscript received: February 27th, 2026; Revised: April 13th, 2026
Approved: May 19th, 2026; Available online: June 23th, 2026; Published: June 23th, 2026.

ABSTRACT - The availability of legacy 2D seismic data in many mature basins offers an opportunity to generate 3D-like subsurface images without the need for expensive 3D seismic acquisition. This study proposes and demonstrates a workflow to construct a pseudo-3D seismic volume from multi-vintage 2D and 3D seismic data in Offshore Southeast Sumatra. The objective is to improve subsurface imaging and depth-structure mapping while minimizing exploration cost and time. Major challenges include variations in amplitude, frequency, phase, and time alignment across datasets acquired with different parameters, as well as determining the optimum line spacing required for reliable 3D reconstruction. The workflow begins with 2D–3D matching and amplitude balancing, followed by spatial interpolation using the 3D Sparse Radon Interpolation technique, which reconstructs coherent reflectors between 2D lines. The generated pseudo-3D volume is then merged with available 3D seismic data to create a unified volume for interpretation. Subsequent time-to-depth conversion is performed using interval velocity data, and the velocity model is iteratively updated using time-preserving tomography based on depth mis-ties between seismic horizons and well markers until convergence is achieved. The resulting depth-structure map provides improved consistency with well control and reveals subtle structural features that are not observed in the individual 2D datasets. The proposed approach demonstrates that pseudo-3D reconstruction from multi-vintage 2D seismic data can serve as a practical and cost-efficient alternative for early-stage exploration and pre-survey evaluation, especially in offshore areas where 3D seismic acquisition is economically constrained.

Keywords: pseudo-3D seismic, multi-vintage 2D data, 3D sparse radon interpolation, depth conversion, time-preserving tomography, Offshore Southeast Sumatra (OSES) Basin.

How to cite this article:

Dadang Ramdan, Abdul Haris, Dewi Manik Darmayanti, Permana Citra Adi, Iwan Rudiyanto, and Muhamad Yanuar Mahardi, 2026, Pseudo-3D Depth Reconstruction from Multi-Vintage 2D and 3D Seismic Data in The Offshore Southeast Sumatra, Scientific Contributions Oil and Gas, 49 (2) pp. 593-608. DOI org/10.29017/scog.v49i2.2110.

INTRODUCTION

In mature basins, such as the Sunda basins, hydrocarbon exploration has become increasingly challenging due to geological complexity and reduced prospectivity. The availability of 3D seismic data is crucial for analyzing geological conditions and mapping the presence of hydrocarbons (Wicaksana, K. S., et al, 2025). Consequently, 3D seismic surveys play a vital role in reducing exploration risk and improving subsurface imaging. However, acquiring new 3D seismic data is both costly and time-consuming. Fortunately, most mature basins possess extensive legacy datasets, including hundreds of 2D seismic lines and well data. These datasets provide an opportunity to reconstruct a 3D-like subsurface model without conducting new 3D seismic acquisition.

Advances in seismic interpolation and data reconstruction techniques have greatly enhanced the use of legacy seismic datasets. Early interpolation approaches were predominantly based on Fourier transform methods, which performed well under regular sampling conditions but were often inadequate for sparsely and irregularly sampled seismic surveys. To overcome these limitations, various approaches have been continuously developed to address data sparsity and improve the reconstruction of incompletely sampled seismic datasets. These developments include transform-domain methods, prediction-filter techniques, sparse reconstruction algorithms, and low-rank approaches, all of which aim to recover missing seismic information while preserving the continuity of geological structures and seismic events.

In addition to seismic reconstruction, accurate structural depth maps are critical for hydrocarbon exploration, as reliable depth positioning directly impacts prospect evaluation, well planning, and reservoir characterization. Accurate structural depth maps are typically generated through pre-stack depth migration (PSDM) or recursive seismic inversion (RSI) (Triyoso, W. et al, 2025), which utilizes shot-gather data and a detailed velocity model. However, when shot-gather data are unavailable, depth conversion of time-migrated seismic data is commonly used as an alternative approach to generate depth maps. However, discrepancies between seismic horizons and well markers are commonly observed due to uncertainties in the velocity model used for time-to -depth conversion. Consequently, velocity model calibration using well-control data is necessary to improve depth-imaging accuracy and structural mapping reliability.

To address these challenges, we propose and demonstrate a workflow for pseudo-3D depth reconstruction that integrates sparse 2D seismic data and well information to generate a coherent pseudo-3D depth volume.

METHODOLOGY

The development of modern seismic interpolation methods, according to Bezzera, Y. S. F., et al., 2021, began with Fourier transform-based approaches, such as minimum weighted norm interpolation (MWNI) (Liu and Sacchi, 2004), Anti Leakage Fourier Transform (ALFT) (Xu, et al., 2005), and Matching Pursuit Fourier Interpolation (MPFI) (Schonewille et al., 2013), which exploit data sparsity in the frequency domain to reconstruct missing traces. Subsequently, other transform-based methods, including Radon and Curvelet transforms, were developed to improve reconstruction performance in more complex geological settings.

More recent advancements have focused on compressed sensing and sparse reconstruction techniques, including 3D sparse radon interpolation (Wang, S., 2017), which achieve higher-quality reconstruction by promoting sparsity through optimization.

3D sparse radon interpolation with ALPRT

3D Sparse Radon Interpolation with Anti-Leakage Parabolic Radon Transform (ALPRT) is an advanced seismic data processing technique that was adapted from Anti-Leakage Fourier Transform (ALFT) (Xu, S. et al, 2005; Schonewille, M. et al, 2009) used to reconstruct missing traces in 3D seismic datasets while minimizing energy leakage in the Radon domain. According to Hollander et al., 2019, the method starts by representing the seismic gather $d(t,x)$ as a combination of multidimensional Radon basis functions. This approximation can be written in the most general form as in Equation 1,

$$\mathrm{d}(t,x) \approx \sum_j m_j \, e^{i2\pi f_j x^2 \cdot \mathrm{p}_j} e^{i2\pi f_j t}, \quad (1)$$

with *t* and *f* denoting the vertical regularly sampled dimension in the time and frequency domains, respectively. Following a preliminary vertical FFT to separate the gather into temporal frequency slices, each slice is approximated as Equation 2,

$$\mathrm{d}(f,x) \approx \sum_j m_j \, e^{i2\pi f x^2 \cdot \mathrm{p}_j} = \mathrm{Am}, \quad (2)$$

where m is the vector of Radon coefficients for a particular frequency *f*. The matrix A contains in its columns the corresponding Fourier basis functions sampled at the irregular 4D spatial grid x , scaled for Radon by itself and by the temporal frequency. $f(x \coloneqq fx^2)$. By applying a sparsity constraint, the algorithm selects only the most significant Radon coefficients to represent seismic events, which helps suppress noise and interpolation artifacts. The Anti-Leakage Parabolic Radon Transform is a matching pursuit approach to find a sparse representation of the form (2). The ALPRT is incorporated to reduce energy spreading between neighboring model parameters, a common problem in conventional Radon transforms due to limited aperture and irregular sampling. This constraint improves the focusing of seismic events in the Radon domain and enhances the stability of the inversion. Sparse Radon Inversion also improves the resolution of the Radon model by employing the L1 norm (Geng, W. et al, 2022) to promote sparsity in the transformed model. As a result, seismic energy is concentrated into a limited number of significant Radon coefficients, reducing smearing artifacts caused by limited data sampling. The objective function of sparse

$$J(m) = \|Lm - d\|_2^2 + \lambda \|m\|_1, \quad (3)$$

inversion can be expressed as Equation 3,
where L denotes the Radon operator, d represents the observed data, m is the Radon model, and λ is the regularization parameter. After estimating the optimal sparse Radon model, the data are transformed back to the space domain to reconstruct missing traces and generate a more regular 3D seismic grid. As a result, this method significantly improves reflector continuity, preserves structural information, and produces higher-quality seismic volumes for subsurface interpretation and pseudo-3D reconstruction.

Time preserving tomography

Time Preserving Tomography (TPT) is a technique that preserves the travel times of seismic events while updating the depth domain horizons and interval velocities by ray tracing (Hong, Y., et al, 2024). TPT aims to incorporate constraints on medium parameters and structure, taken from geological knowledge or well marker information, into the tomographic solution. TPT is implemented in structural model-based tomography, keeping the refined models tied to the structure as shown in Figure 2. The fundamental equation of TPT can be written as Equation 4,

$$0 = \delta t = \sum i(A_v \Delta V + A_\varepsilon \Delta\varepsilon + A_\delta \Delta\delta + A_z \Delta Z) \quad (4)$$

where ΔV denotes the velocity change, $\Delta\varepsilon$ and $\Delta\delta$ represent the changes in the anisotropic parameters epsilon and delta, respectively, and ΔZ denotes the change in horizon depth.

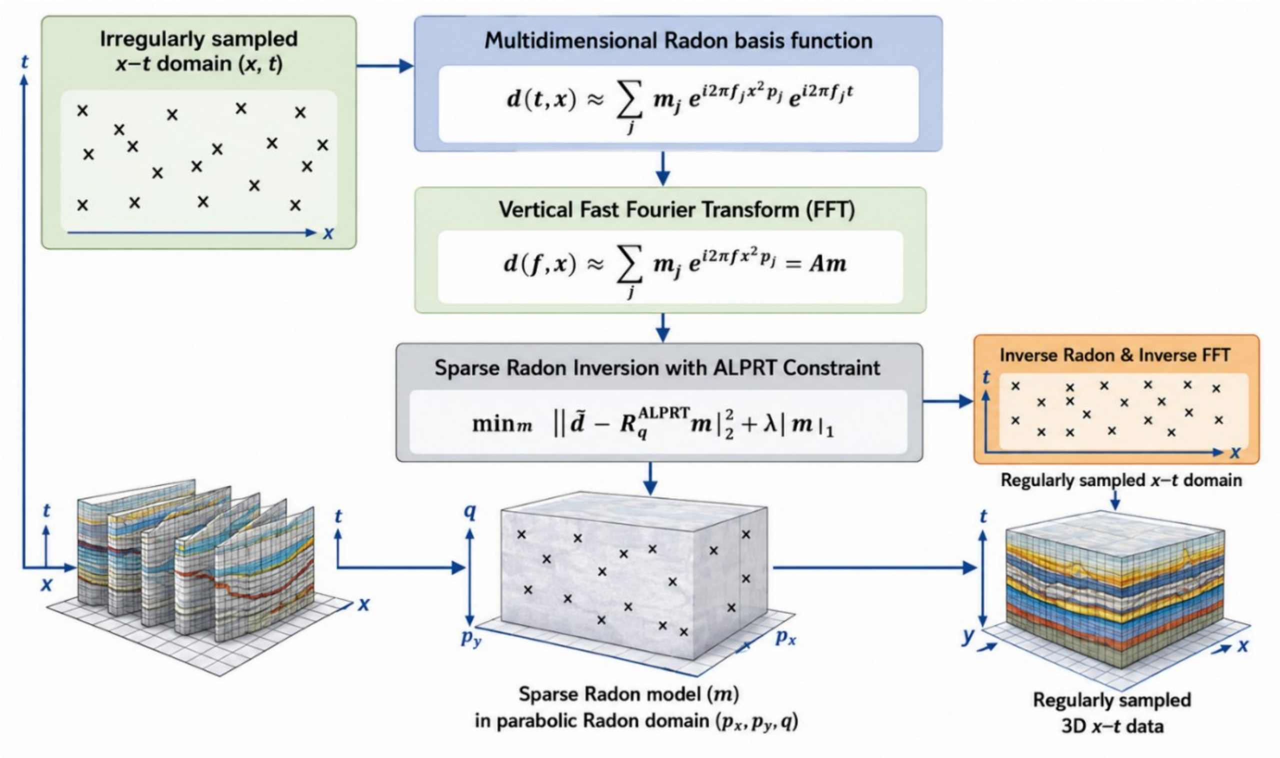

Figure 1. The schematic workflow of 3D sparse parabolic Radon interpolation with ALPRT inversion methods was adapted from Hollander & Yilmaz 2019).

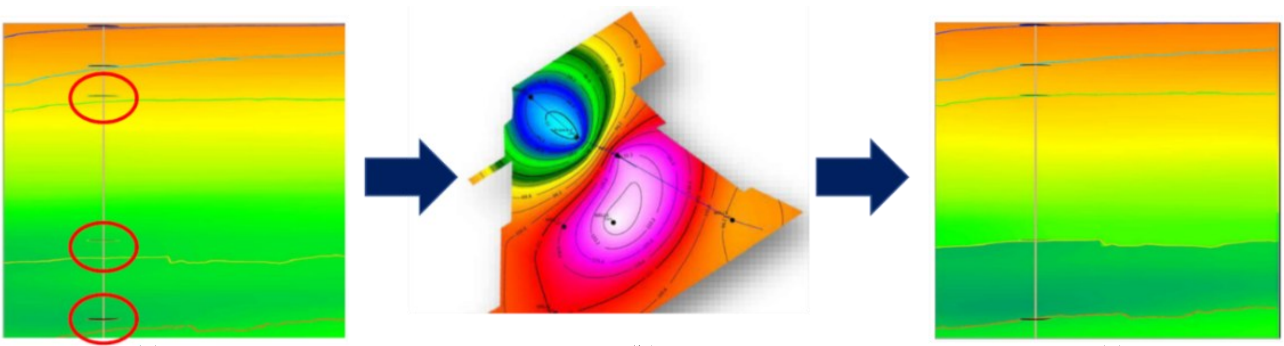

Figure 2. Conceptual illustration of Time Preserving Tomography (TPT).
The depth mismatch between the seismic horizon and well markers (a) is converted into a depth-mismatch map (b) and incorporated into the TPT formulation, allowing the model to be updated while preserving structural consistency with the well data(c). (modified from Rob, M., 2015)

Data description

The study area, shown in Figure 3, is located north of Jakarta, in Offshore Southeast Sumatra. The input dataset consists of:

- 148 multi-vintage 2D PSTM stack seismic lines
- 138 2D RMS velocity lines
- One 3D PSTM stack seismic volume
- One 3D RMS velocity volume
- Five wells containing sonic, density, and formation markers.

The multi-vintage 2D seismic dataset consists of ten surveys acquired using different acquisition parameters, as summarized in Table 1. Continuous advancements in seismic acquisition technology have enabled the efficient collection of increasingly large volumes of seismic data, thereby improving the quality and spatial coverage of subsurface imaging.

The workflow

The workflow used in this study was developed based on methodologies previously described by Whiteside et al. (2013), O'Keefe et al. (2017), Humberto et al. (2018), and Abdullah (2022), with several modifications introduced to accommodate the characteristics of the available dataset and the objectives of the present study. The workflow, as shown in Figure 4, is divided into two stages. Stage I focuses on pseudo-3D reconstruction. It begins with seismic matching analysis and rebinning into a new pseudo-3D survey geometry, followed by 3D post-stack interpolation. After the pseudo-3D volume is generated, it is merged with the existing 3D seismic data and is ready for interpretation.

The interpretation process begins with the generation of a synthetic seismogram from sonic and density logs, which is then convolved with a wavelet. Stretching and squeezing are subsequently applied to calibrate the synthetic seismogram to the seismic section. This process is iteratively performed until the maximum correlation coefficient between the synthetic seismogram and seismic data is achieved.

Stage II focuses on velocity model building. The process begins with time-to-depth conversion using an initial interval velocity model. This interval velocity model is updated using the time-preserving tomography method based on the mis-depth information between the interpreted seismic horizons and well markers. The process is performed iteratively until

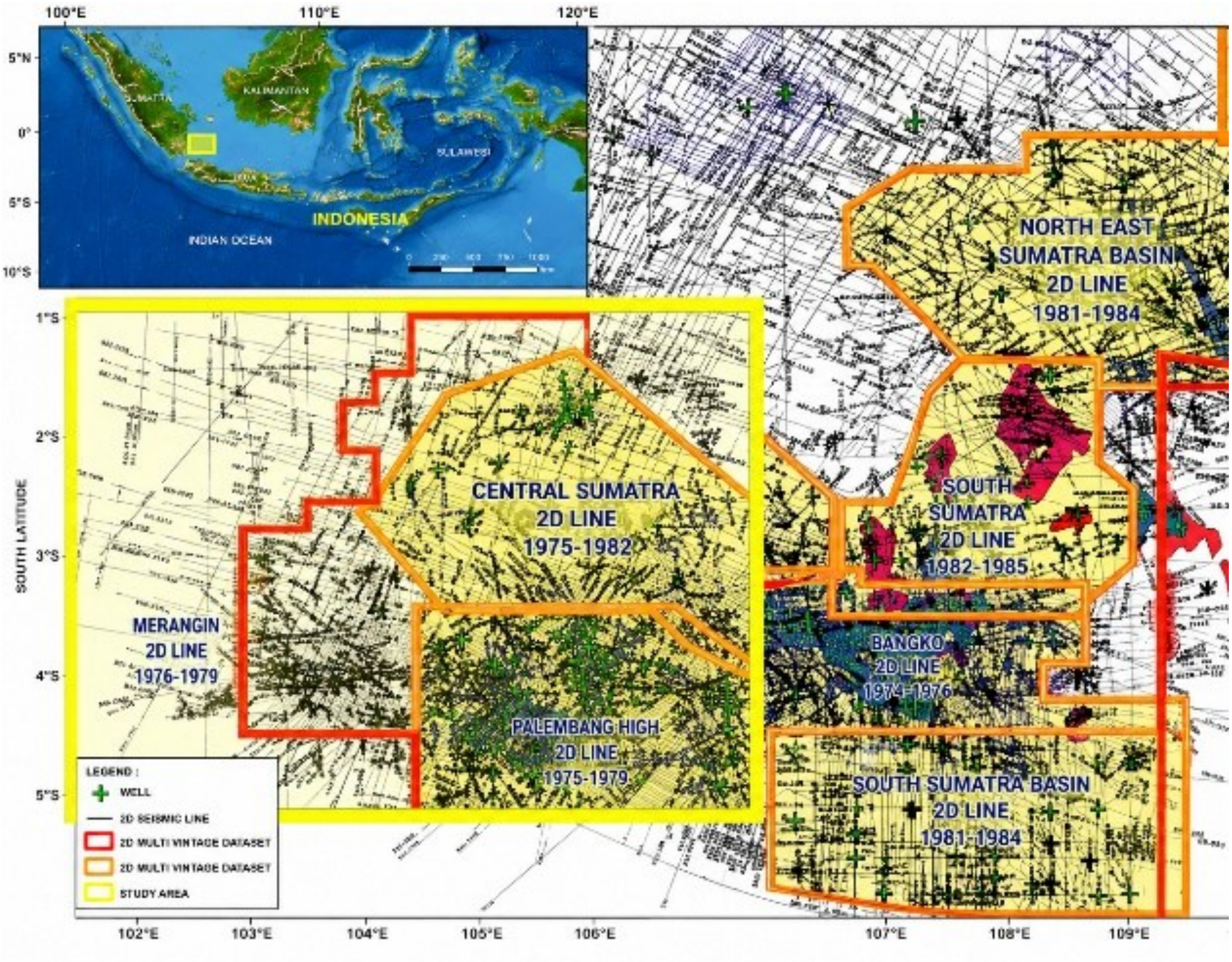

Figure 3. Study area highlighted by the yellow box, comprising a dozen 2D multi-vintage seismic lines (black) and a 3D seismic survey (orange) (modified from Ralanarko et al., 2011).

Table 1. Summary of acquisition parameters for ten multi-vintage 2D seismic surveys used in this study

Vintage	80	81	82	83	87	89	90	91	93	94
Number of Channels	48	48	48	48	60	192	240	192	240	240
Source Interval (m)	25	25	25	25	26.6	26.6	25	25	25	25
Group Interval (m)	25	25	25	25	26.6	13.3	12.5	12.5	12.5	12.5
Delay time (ms)	61.2	51.2	51.2	0	16.43	0	0	51.2	51.2	115
Near offset (m)	150	87	135	100	134	118.2	150.3	143	130	108
Source depth (m)	7.8	7	7	5.6	6	6	5	5	5	5
Receiver depth (m)	8	7	7	6	6	6	6	5	5	6

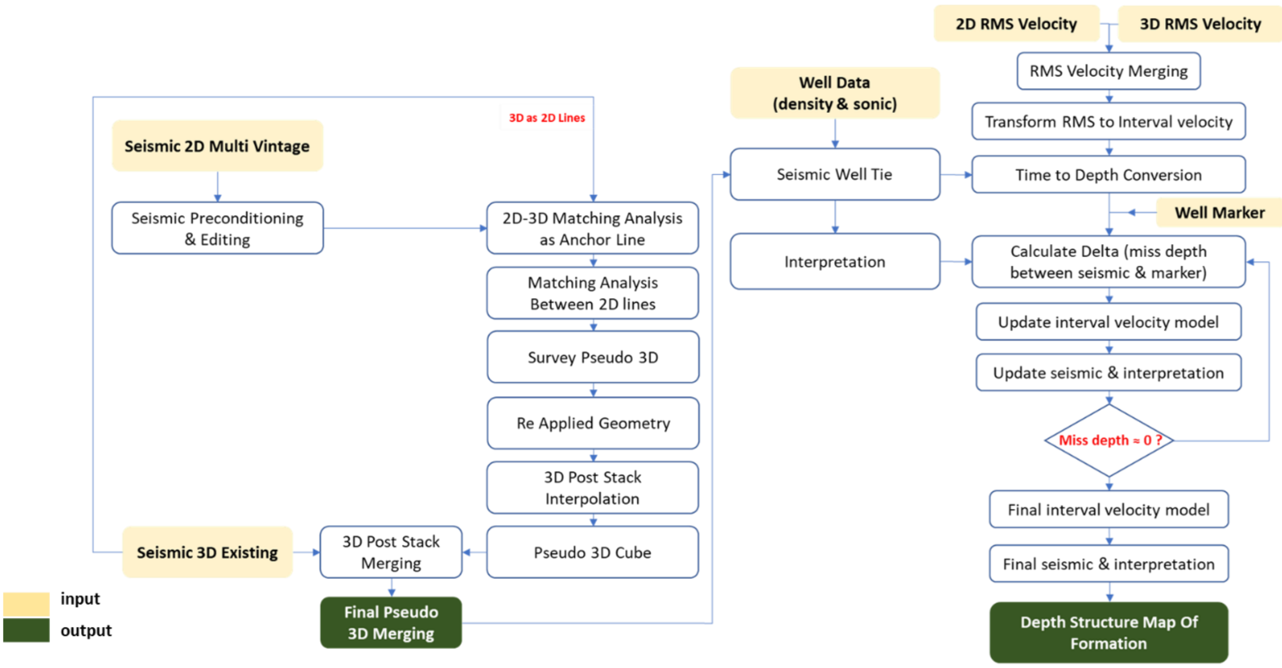

Figure 4. Workflow of pseudo 3D depth reconstruction

convergence is achieved.

RESULT AND DISCUSSION

Seismic matching analysis

The seismic matching analysis functionality is used to identify seismic mis-ties between seismic sections (Abdullah, A., et al, 2022). After the calculations are completed, as shown in Figure 5a, the resulting mis-tie values of amplitude, phase, and time shift are displayed in tabular form and then applied to the seismic sections. To control and evaluate the process, the results can be visualized in correlation windows. The maximum cross-correlation value is obtained when the time shift is zero. For frequency matching, band-pass filtering is applied to adjust the frequency content between the datasets. Matching analysis is a crucial step in the workflow to ensure consistency between 2D lines. It is done line by line to ensure the interpolation process produces a reliable and coherent seismic volume.

After seismic matching analysis, the maximum correlation has a time shift value around zero, and the sections have the same frequency trend, as shown in Figure 5b.

Pseudo 3D reconstruction

Figure 6a shows an example of the pseudo-3D reconstruction. Real 3D seismic data are shown on the left and right sides, and the pseudo-3D area is shown in the middle. The pseudo-3D area comprises seismic lines with 50–1000 m spacing. The pseudo-3D area exhibits strong spatial aliasing and trace gaps, resulting in discontinuous and noisy reflectors. Figure 6b shows a significantly improved seismic image of the missing traces obtained by interpolation and reflector continuity. Demonstrating that 3D sparse Radon interpolation recovers structural information and greatly facilitates seismic interpretation compared with pre -interpolated data. The impact of regularizing the section for interpretability allows the horizon interpretation to be interpreted more smoothly and confidently from point A to B. The interpretation becomes more geologically consistent.

Interval velocity model building using TPT

Figure 7a presents an initial pseudo-3D depth seismic section overlaid with an initial interval velocity model and well data markers, illustrating the relationship between seismic reflectors and actual well-based depth references. The initial pseudo-depth section is produced from time-to-depth conversion using the interval velocity. The colored horizons represent the interpreted seismic events, and the vertical markers indicate the well positions and their corresponding depth picks. A clear depth mismatch can be observed between the pseudo-depth seismic reflectors and the well markers in the highlighted (red box) and zoomed-in area on the right, where the seismic horizons do not perfectly align with the known formation tops from the wells. This discrepancy may indicate inaccuracies in the velocity model or limitations in the pseudo-depth conversion process, resulting in the mispositioning of subsurface structures. Overall, the image emphasizes the need for further calibration, such as velocity updating or depth refinement, to better tie the seismic data with well control and improve geological reliability. Figure 7b shows a pseudo-3D depth seismic section that has been tied to well data markers, demonstrating improved alignment between seismic reflectors and well-known formation depths from wells. Compared with an untied section, the highlighted and zoomed-in area reveals that the seismic horizons now more closely match the well markers, reducing the previous depth mismatch as shown in Figure 8. This improved correlation that the depth model has been calibrated, likely through velocity updating or well-based correction, resulting in more accurate positioning of geological structures. Overall, the image emphasizes the importance of well ties in validating and refining pseudo-depth seismic interpretations to achieve higher confidence in subsurface mapping.

Optimum line spacing for pseudo 3D reconstruction

What is the optimum reliable line spacing for pseudo 3D reconstruction? To answer this question, we conducted an experiment using a 3D seismic dataset by systematically subsampling a full 3D seismic dataset at varying distances, as shown in Figure 9. The original (legacy) 3D data were treated as the reference, and pseudo-3D sections were generated using different input spacings (125 × 125 m, 250 × 250 m, and 500 × 500 m).

The structural fidelity of each reconstructed section is then quantitatively evaluated using the Structural Similarity Index (SSIM) by metadata2go.com, which measures how closely each pseudo-3D result resembles the original 3D image. SSIM is an image quality metric proposed by Wang et al. (2004) to evaluate the similarity between two images based on structural information rather than pixelwise errors. SSIM assesses image similarity by considering luminance, contrast, and structural components, resulting in a measure that is more consistent with human visual perception.

As shown in Figure 9, denser spacing (125×125 m) preserves structural features more accurately, yielding higher similarity, whereas increasing the spacing leads to progressive degradation in the continuity and resolution of reflectors, reflected by lower SSIM values. This comparison demonstrates that the optimum spacing should balance acquisition efficiency and structural reliability, with closer spacing providing more accurate

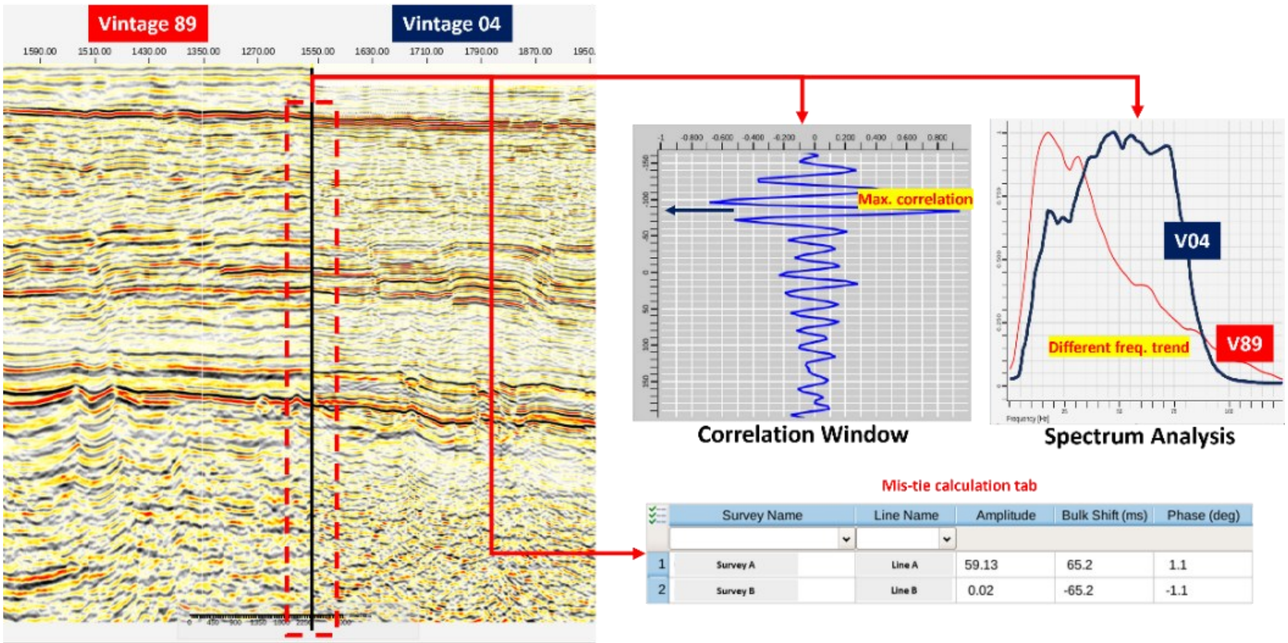

(a)

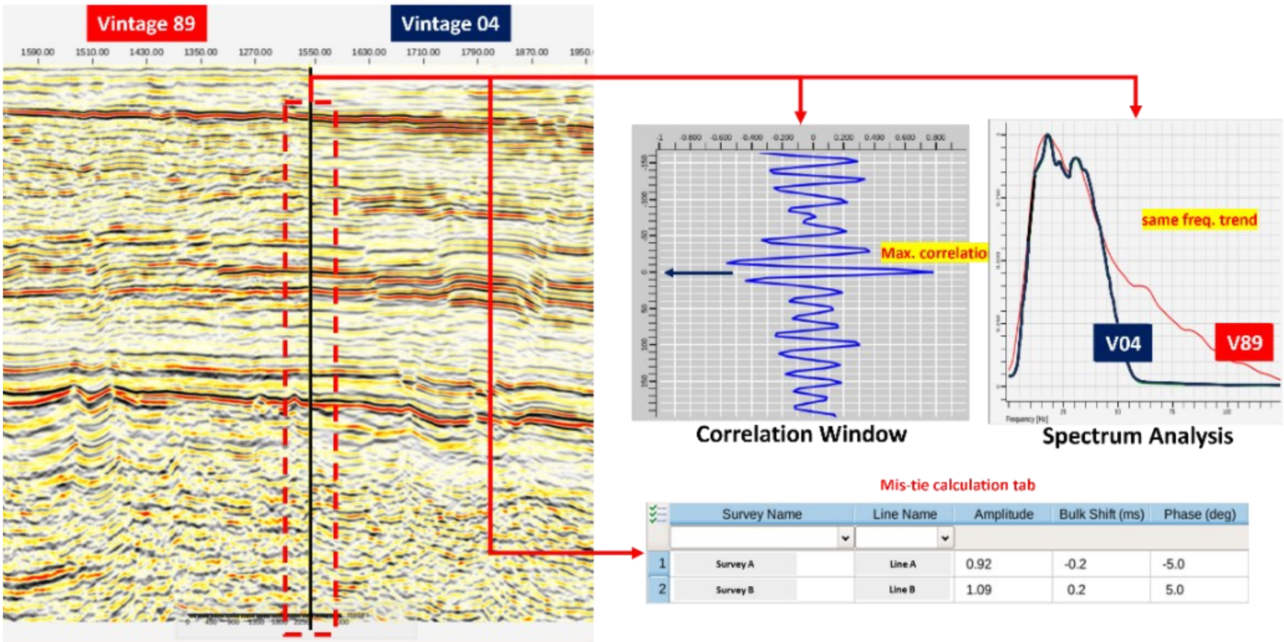

(b)

Figure 5. Seismic matching analysis showing (a) before and (b) after mis-tie correction.
The correction ensures consistency among the seismic datasets in terms of amplitude, phase, time, and frequency.
An optimal correlation window is achieved when the time shift approaches zero and the frequency spectra of the datasets exhibit similar trends.

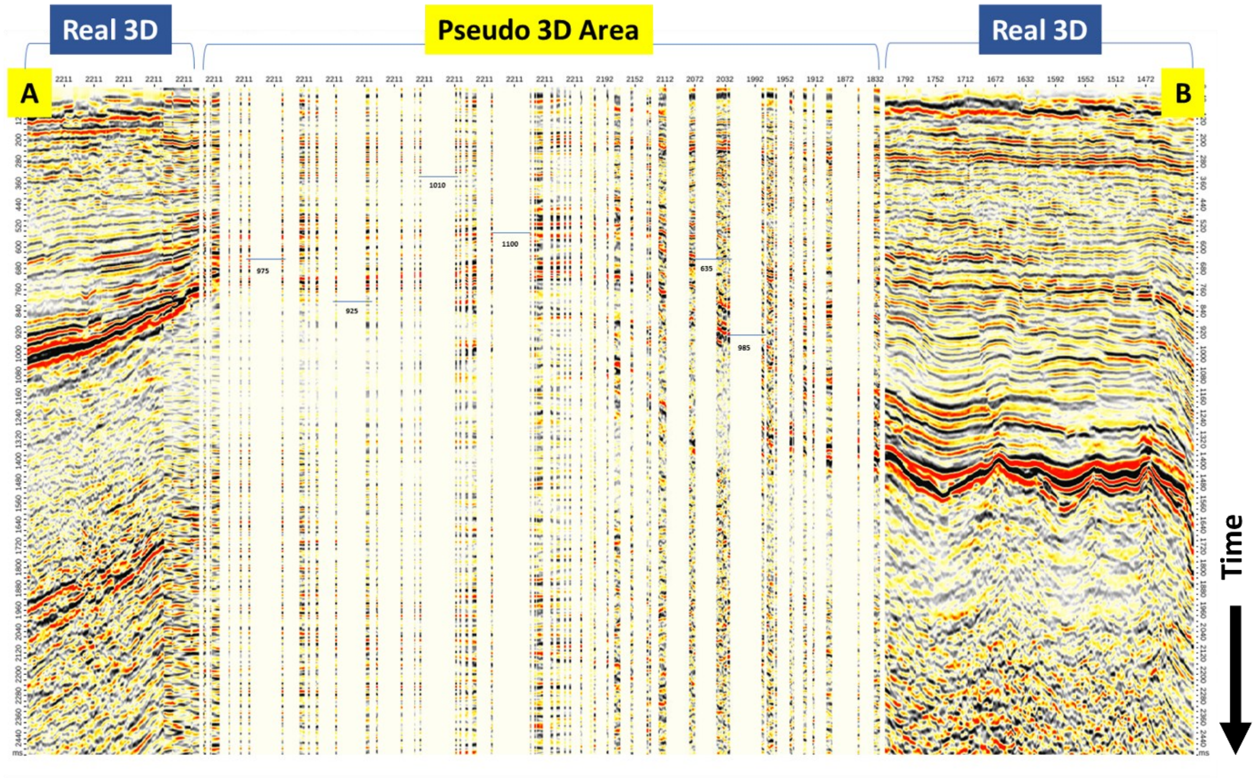

(a)

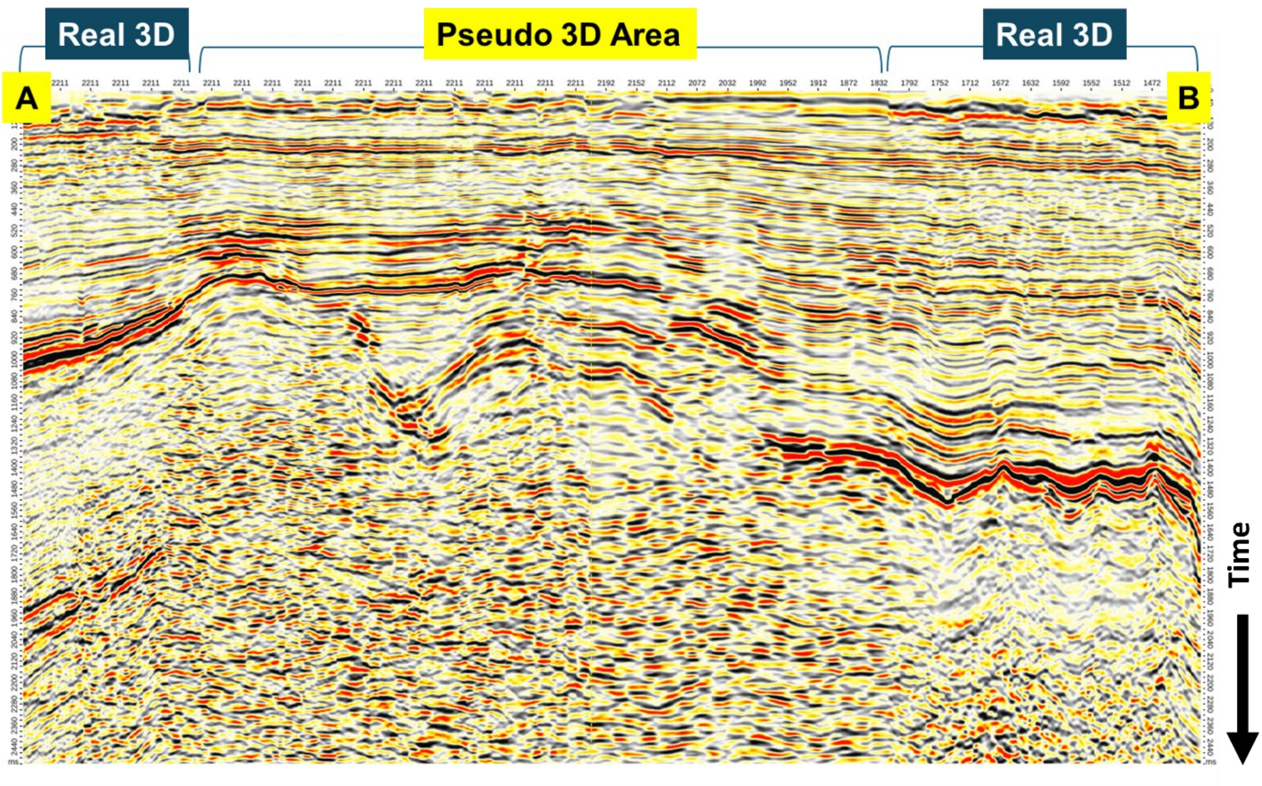

(b)

Figure 6. (a) Traverse line across existing 3D seismic and pseudo-3D reconstruction areas. The pseudo-3D region contains missing traces with spacing varying from 50 to 1000 m. (b) The missing traces were reconstructed after 3D post-stack interpolation using 3D Sparse Radon Interpolation, producing a continuous seismic image and revealing a carbonate structure or body that was not previously visible.

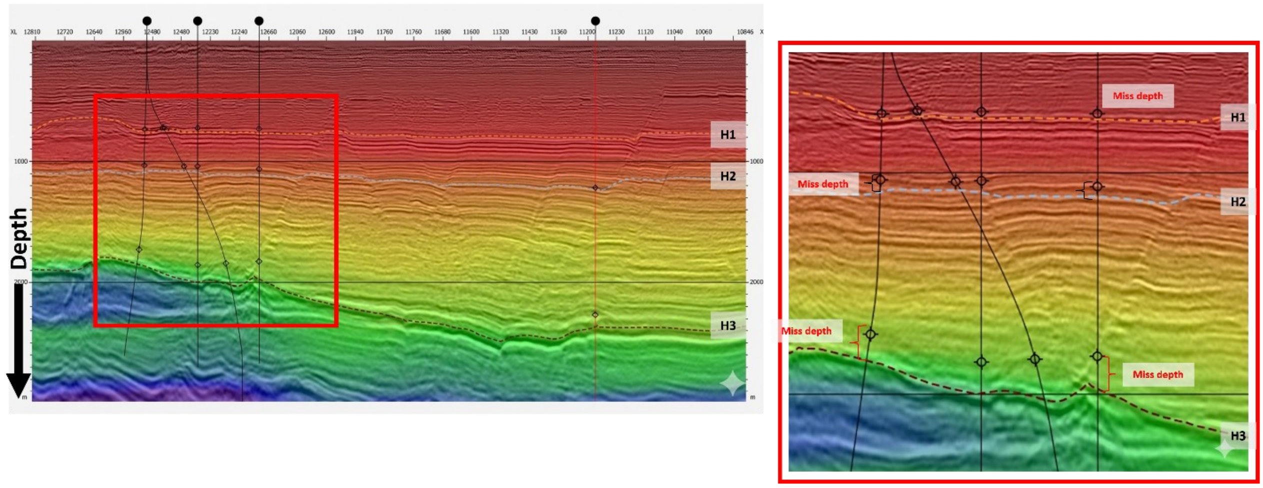

(a)

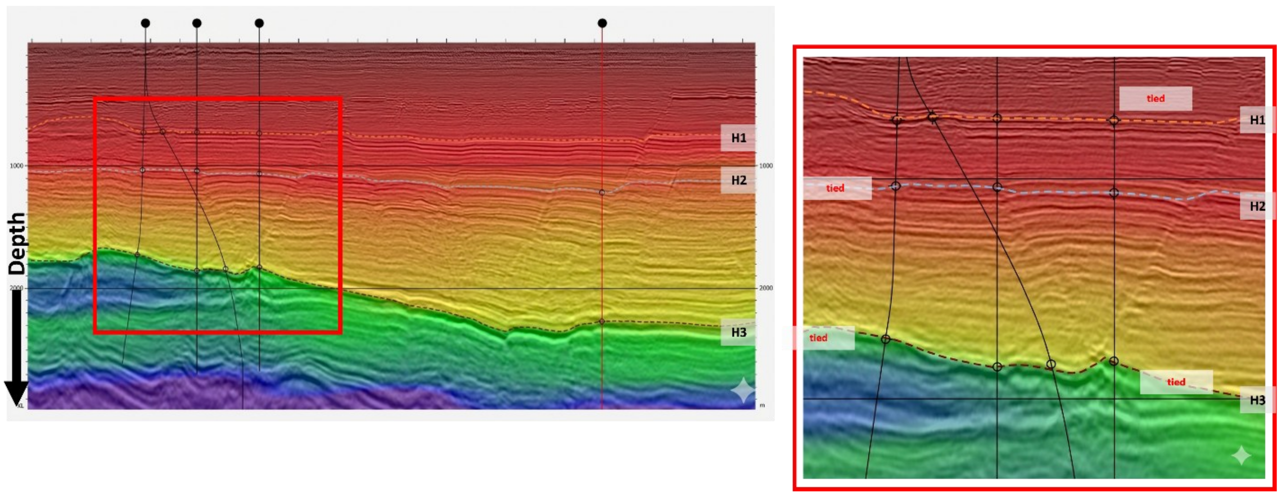

(b)

Figure 7. (a) The traverse line across the well location shows a depth between the initial pseudo 3d depth section and the well marker data, and (b) the pseudo depth section is tied to the well marker data.

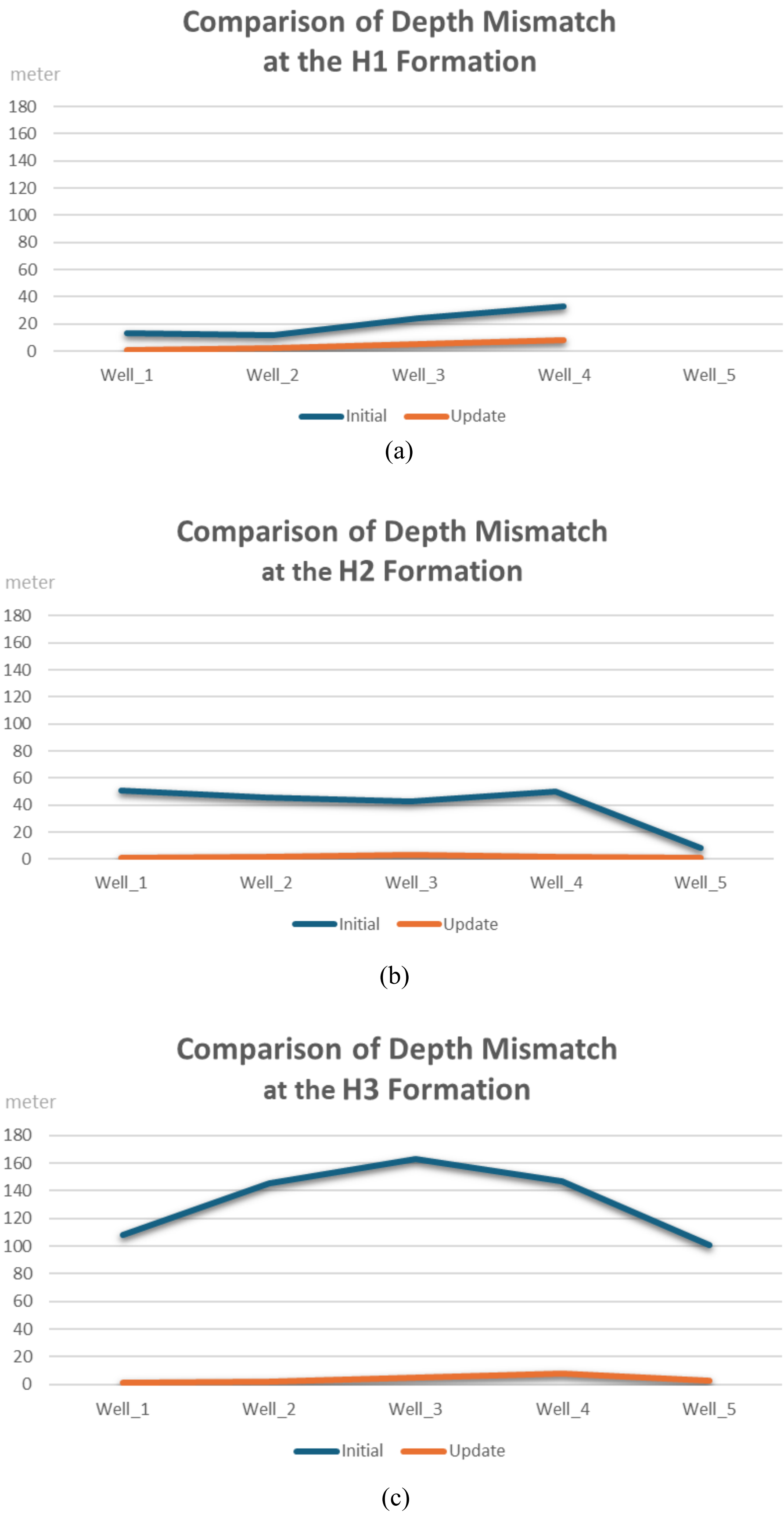

Figure 8. Comparison of depth mismatch before (blue) and after (orange) velocity model updating for the H1 (a), H2 (b), and H3 (c) formations. The reduced mismatch after updating indicates improved depth-model accuracy.

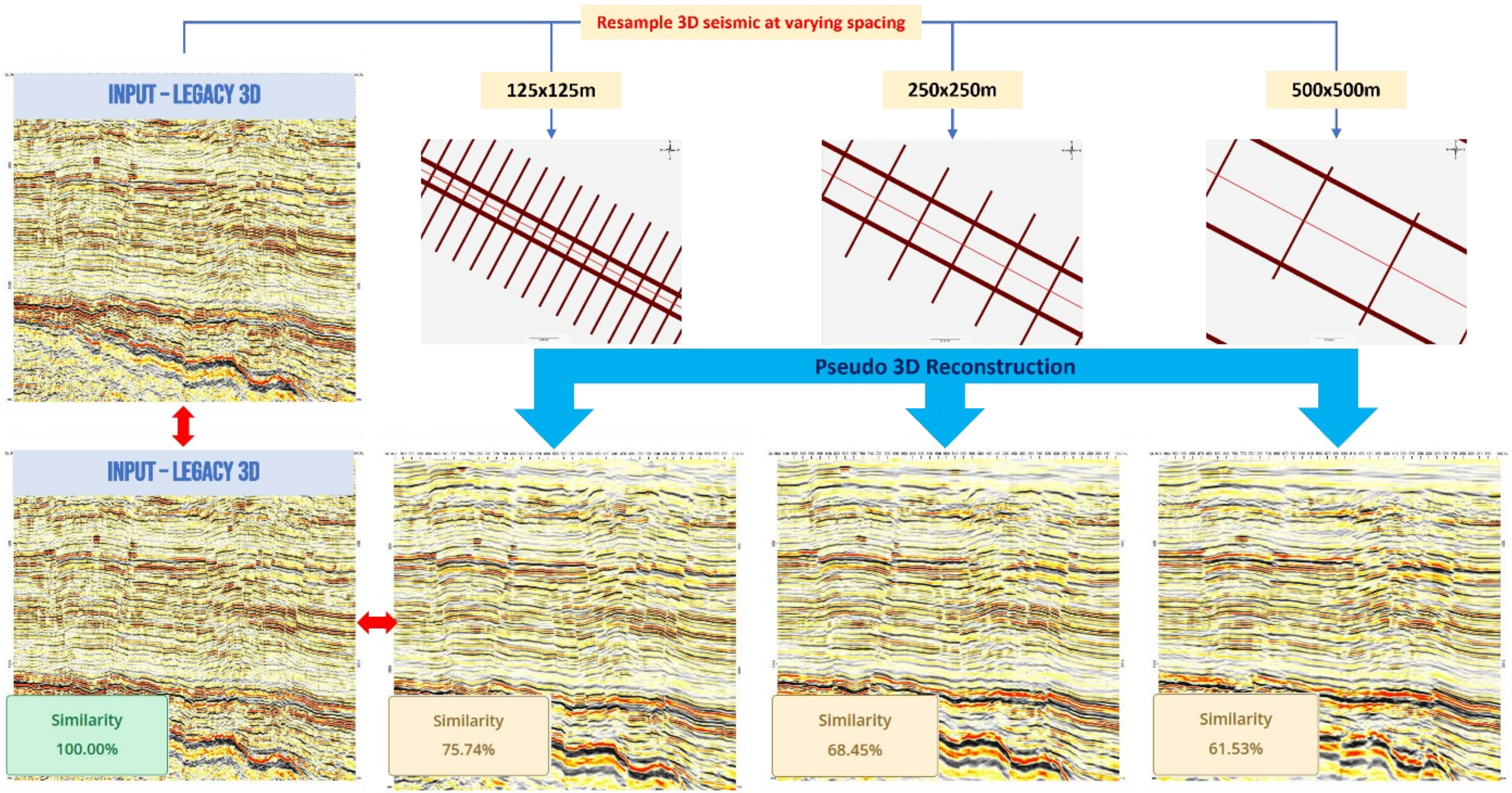

Figure 9. Structural similarity index (SSIM) comparison between pseudo-3D volumes generated from varying line spacings and the legacy 3D seismic volume. Higher SSIM values indicate greater similarity between the compared seismic images. Higher similarity scores indicate the two images were the same and vice versa

pseudo-3D reconstruction.

Limitation

The 3D sparse Radon interpolation method has several limitations. The reconstruction result is strongly dependent on the input line spacing, where wider spacing may reduce the interpolated pseudo-3D volume's reliability. This is in line with another previous study by Humberto, P. et al. (2018). Furthermore, the sparsity regularization applied in the inversion process may cause a loss of absolute amplitude and introduce amplitude distortion, making the method unsuitable for quantitative seismic analyses such as amplitude-based interpretation.

The Time Preserving Tomography (TPT) method also has several limitations. The accuracy of the updated velocity model is highly dependent on the availability and distribution of well data used as calibration references. Furthermore, the method cannot directly resolve anomalous velocity effects, such as pull-up effects, because the velocity update process mainly relies on mis-depth information between seismic interpretation and well markers.

In addition to the two abovementioned points, the frequency matching step in the workflow may cause a loss of high-frequency content, as shown in Figure 10, due to the balancing of frequency content between the datasets. An additional processing step is recommended to overcome this issue and obtain more robust results, as shown in Figure 11. First, the 2D multivintage seismic data should be reprocessed from the raw gathers using consistent processing parameters across all datasets. The pseudo-3D depth reconstruction workflow can be applied after the PSTM

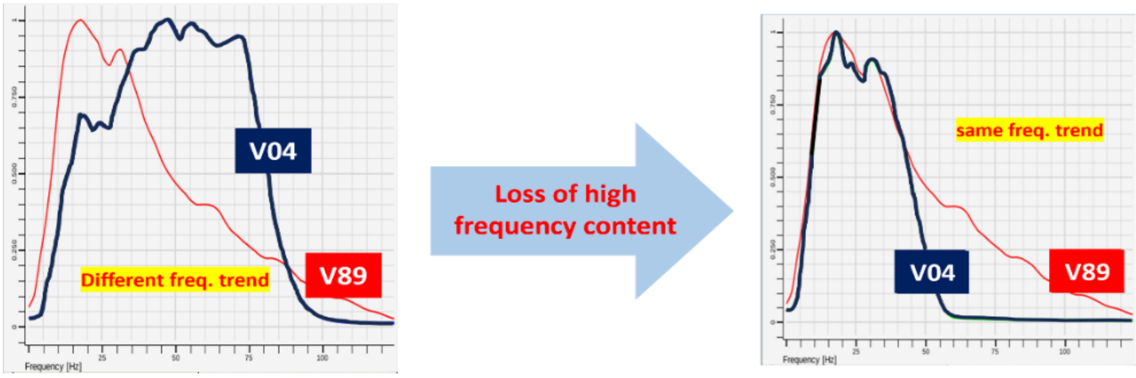

Figure 10. Frequency matching between seismic datasets of different vintages. The dataset represented by the blue spectrum contains higher-frequency content than the red spectrum and is therefore subjected to a high-cut filter to achieve spectral consistency, resulting in the loss of high-frequency energy.

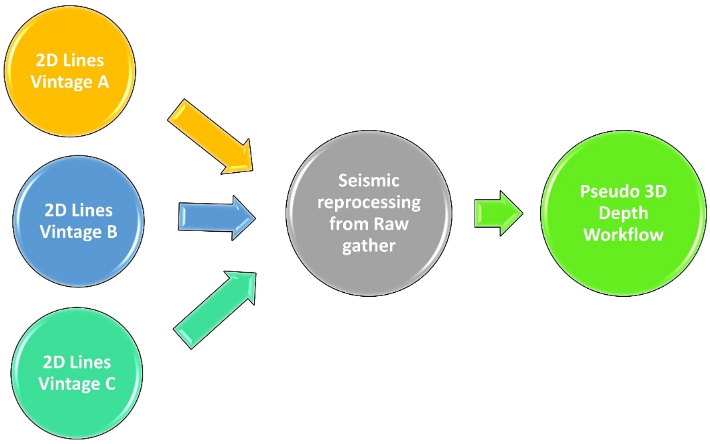

Figure 11. An additional workflow is proposed to achieve more robust and reliable results. In this approach, the multi-vintage 2D seismic datasets should be reprocessed from the raw gathers using a consistent processing sequence and parameters across all surveys before proceeding with the pseudo-3D depth reconstruction workflow. This would improve data consistency, minimize vintage-related discrepancies, and enhance the quality of the reconstructed pseudo -3D depth volume.

sections are generated.

CONCLUSION

In conclusion, the proposed pseudo-3D depth reconstruction workflow has demonstrated its effectiveness in enhancing the value of sparse multi -vintage 2D seismic datasets. The results show that seismic matching analysis is a crucial step in the workflow to produce coherent 2D seismic lines.

3D sparse Radon interpolation methods successfully reconstruct coherent 2D seismic lines into consistent pseudo-3D seismic volumes.

An optimum line spacing of 100-250 m provides reliable pseudo-3D reconstruction, achieving a structural similarity index (SSIM) score exceeding 68% relative to the legacy 3D reference data.

Time-preserving tomography successfully generated a reliable velocity model, as demonstrated by the pseudo-depth section, which exhibits strong correlation and accurate tying with well marker data.

ACKNOWLEDGMENT

The author would like to express sincere appreciation to Prof. Dr. rer. nat. Abdul Haris for his invaluable guidance and supervision throughout this study. The author also gratefully acknowledges PT. Pertamina EP for providing the data, computational facilities, and permission to publish this work.

DECLARATIONS

Author contribution

D. Ramdan: conceptualization, methodology, data processing, data curation, data analysis, visualization, writing original draft, writing review & editing. A. Haris: Supervision (co), methodology, validation, writing review & editing. D.M. Darmayanti: Supervision (co), data collecting, seismic interpretation, writing review. P.C. Adi: Supervision (co), writing review. I. Rudiyanto: Supervision (co), data access authorization. M. Y. Mahardi: Supervision (co), data access authorization.

Funding statement

The authors declare that they have no known competing financial interests or personal relationships that could have influenced the work reported in this paper.

Competing interest

The authors declare that they have no known competing financial interests or personal relationships that could have influenced the work reported in this paper.

The use of AI or AI-assisted technologies

The author(s) used ChatGPT to assist. After using this tool, the authors review and edit the content as needed and take full responsibility for the publication's content

Terms & Symbols	Definition	Unit
ALPRT	Anti-leakage parabolic radon transform	
MWNI	Minimum weighted norm Interpolation	
OSES	Offshore southeast sumatra	
PSTM	Pre-stack Time Migration	
PSDM	Pre-stack Depth Migration	
RMS	Root mean square	
SSIM	Structural similarity index	
SSA	Singular spectrum analysis	
TPT	Time preserving tomography	

GLOSSARY OF TERMS AND SYMBOLS

REFERENCES

Abdullah, A. & Basyuni, S., (2022), Pseudo 3D Seismic Generation From Multi-Vintage 2D and 3D Seismic data for Hydrocarbon Exploration at Eastern Indonesian Basin, Indonesian Petroleum Association 46th CONVEX, Jakarta: 21-23 September 2022, ISBN: 978-602-8601-

28-3.

Bevc, D., Neodorub, O., Hollander, Y., & Yilmaz, O., (2019), An acceleration method for the anti-leakage parabolic Radon transform for seismic data interpolation, SEG Technical Program Expanded Abstract 2019, https://doi.org/10.1190/segam2019-3199275..

Bezerra, Y. S. F., Garabito, G., and Sacchi, M. D., (2021), A comparative study of multidimensional Fourier reconstruction of 2D prestack seismic data', Journal of Applied Geophysics,https://doi.org/10.1016/j.jappgeo.2021.104445.

Geng, W., Li, J., Chen, X., Ma, J., Xu, J., Zhu, G. and Tang, W, (2022), 3D high-order sparse radon transform with L1–2 minimization for multiple attenuation, Geophysical Prospecting, 70: 655-676. https://doi.org/10.1111/1365-2478.13185.

Hong, Y., Cambois, G., Al Neyadi, A. A., Cowell, J., Aljaberi, F., Al Kaabi, A. S., & Puri, A. K., (2024), Time-Preserving Tomography in Structure Mapping: A Case Study of a Deep Gas Reservoir, Offshore Abu Dhabi. Abu Dhabi International Petroleum Exhibition & Conference 2024, Abu Dhabi: 4-7 November 2024, https://doi.org/10.2118/222921-M.

Humberto, P., Neves, F., Caerio, M. H., & Gomes, J., (2018), First Abu Dhabi 2D/3D Seismic Merge. Fast Track Approach For Seismic Data Integration at Regional Scale in Exploration Studies, Abu Dhabi International Petroleum Exhibition & Conference 2018, Abu Dhabi: 12-15 November 2018, https://doi.org/10.2118/193066-M.

Metadata2Go, (2026), Metadata2Go: Online metadata and image analysis tool, QaamGo Web GmbH. Metadata2G.com, Accessed March 19, 2026.

O'Keefe, S., Ratnett, N., Woodburn, N., Pedersen, C., Bradbury, W., Guo, M., and Whiteside, W., (2018), The development and applicability of structurally conformable 2D to 3D interpolation, SEG International Exposition and 87th Annual Meeting, Houston: 24-29 September 2017, https://doi.org/10.1190/segam2017-17723357.

Ralanarko, D., Wahyuadi, D., Nugroho, P., Rulandoko, W., Syafri, I., Almabrury, A., and Nur, A, A., (2020), Seismic Expression of Paleogene Talangakar Formation – Asri & Sunda Basin, Java Sea, Indonesia, Berita Sedimentology : Indonesian Journal of Sedimentary Geology, Vol 46, No 1.

Robb, M., (2015), Time Preserving Tomography (TPT) - Velocity Refinement through Tomographic Depthing, Paradigm Gephysical

Schonewille, M., Klaedtke, A., Vigner, A., Brittan, J., & Martin, T., (2009), Seismic data regularization with the anti-alias anti-leakage Fourier transform, First Break 27(9): 85-92. https://doi.org/10.3997/1365-2397.27.1304.32570.

Triyoso, W., & Hutapea, F. L., (2025), The Use of the Common Offset of the Common Reflection Surface (CO-CRS) for Velocity Analysis and Data Preconditioning. *Scientific Contributions Oil and Gas*, 48(4), 165-177. https://doi.org/10.29017/scog.v48i4.193.

Wang, Y., Gong, X., & Hu, B., (2024), Seismic Data Reconstruction Using a Phase-Shift-Plus-Interpolation-Based Apex-Shifted Hyperbolic Radon Transform, Remote Sens. 2024, 16, 1114. https://doi.org/10.3390/ rs16071114.

Wang, S., Li, J., Xue, Y., Zhou, Y., & Ma, X., (2017), AVO-Preserving Data Reconstruction by 3D High-Order Sparse Parabolic Radon Transform, SEG International Exposition and 87th Annual Meeting, Houston.

Wang, Z., Bovik, A. C., Sheikh, H. R., & Simoncelli, E. P., (2004), Image quality assessment: from error visibility to structural similarity, IEEE Transactions on Image Processing, Vol. 13, 600-612, https://doi.org/10.1109/ TIP.2003.819861.

Whiteside, W., Wang, B., Bondeson, H., & Li, Z., (2013), Enhanced 3D Imaging from 2D Seismic Data and its Application to Surveys in the North Sea, EAGE Conference & Exhibition incorporating SPE EUROPEC, London: 10-13

June 2013.

Wicaksana, K. S., Pasaribu, D., & Purba, H., (2025), Structural Configuration And Paleogeography of The Krishna Field in The Sunda Basin. Scientific Contributions Oil and Gas, 48(4), 463-487. https://doi.org/10.29017/scog.v48i4.1964.

Xu, S., Zhang, Y., Pham, D., & Lambare, G., (2005), Antileakage Fourier transform for seismic data regularization', Geophisic, Vol. 70, No. 4 (July-August 2005); P. V87-V95, 17 FIGS. https://doi.org/10.1190/1.199371.